

Targeting Dyrk1A with AAVshRNA Attenuates Motor Alterations in TgDyrk1A, a Mouse Model of Down Syndrome

Jon Ortiz-Abalia,^{1,2} Ignasi Sahún,^{1,2} Xavier Altafaj,^{1,2} Núria Andreu,^{1,2} Xavier Estivill,^{1,3} Mara Dierssen,^{1,2} and Cristina Fillat^{1,2,*}

Genetic-dissection studies carried out with Down syndrome (DS) murine models point to the critical contribution of Dyrk1A overexpression to the motor abnormalities and cognitive deficits displayed in DS individuals. In the present study we have used a murine model overexpressing Dyrk1A (TgDyrk1A mice) to evaluate whether functional CNS defects could be corrected with an inhibitory RNA against Dyrk1A, delivered by bilateral intrastriatal injections of adeno-associated virus type 2 (AAVshDyrk1A). We report that AAVshDyrk1A efficiently transduced HEK293 cells and primary neuronal cultures, triggering the specific inhibition of Dyrk1A expression. Injecting the vector into the striata of TgDyrk1A mice resulted in a restricted, long-term transduction of the striatum. This gene therapy was found to be devoid of toxicity and succeeded in normalizing Dyrk1A protein levels in TgDyrk1A mice. Importantly, the behavioral studies of the adult TgDyrk1A mice treated showed a reversal of corticostriatal-dependent phenotypes, as revealed by the attenuation of their hyperactive behavior, the restoration of motor-coordination defects, and an improvement in sensorimotor gating. Taken together, the data demonstrate that normalizing Dyrk1A gene expression in the striatum of adult TgDyrk1A mice, by means of AAVshRNA, clearly reverses motor impairment. Furthermore, these results identify Dyrk1A as a potential target for therapy in DS.

Introduction

Down syndrome (DS [MIM 190685]) is a multisystem disorder resulting from the presence of an extra copy of the human chromosome 21 (HSA21, *Homo sapiens* auto-some 21). Although HSA21 contains more than three hundred genes, those contributing to DS phenotypes are likely to be considerably less.¹ In fact there is a current debate regarding whether few genes with a strong impact might be participating in a given phenotype or whether such a phenotype will result from the impact of multiple genes with modest effects. Interestingly, the genes implicated in the trisomy are nonmutated genes, and thus it is only 50% overexpression that contributes to the overall effects.²

DYRK1A [MIM 600855], one of the triplicated genes in trisomy 21, has been demonstrated to be 1.5-fold overexpressed in DS brains, both at transcript and protein levels, indicating that this protein is overexpressed in a gene-dosage-dependent manner.^{3,4} *DYRK1A* encodes for dual-specificity tyrosine-(Y)- phosphorylation regulated kinase 1A, an enzyme defined as dual-substrate specific because it autophosphorylates on Tyr-321 and in Ser/Thr and phosphorylates target proteins on serine/threonine residues.⁵ A variety of substrates and interacting proteins have been described,⁶ suggesting that *DYRK1A* may be participating in multiple biological pathways. Functional evidences revealing the contribution of *DYRK1A* overexpression in a DS phenotype comes mainly from studies on different genetically engineered mice. In this respect, transgenic mice overexpressing Dyrk1A display cognitive deficits

and motor abnormalities,^{7–10} as well as vascular defects.¹¹ All these evidences suggest that strategies directed toward reducing Dyrk1A overexpression might be considered as a potential approach to correct specific DS phenotypic alterations dependent on Dyrk1A overexpression. The specific inhibition of Dyrk1A could be achieved by the use of small interfering RNA (siRNA) approaches, employing an efficient delivery system that targets neuronal cells. Adeno-associated viruses have been shown to effectively deliver genes and shRNA sequences to the CNS, thereby mediating long-term transgene expression with limited immune response.¹²

In the present study, we explore the possibility that by subtly reducing Dyrk1A in the brain of adult TgDyrk1A mice by adeno-associated virus delivery of an shRNA sequence specific for Dyrk1A, it may be feasible to correct the motor abnormalities present in these mice.

Material and Methods

Plasmid Constructs

pU6-shDyrk1A and p-U6scDyrk1A were generated as follows: A sh1073Dyrk1A sequence was designed to target 1073–1083 bp within the rat Dyrk1A open reading frame. The sc1073Dyrk1A sequence consisted of a scrambled version of the sh1073Dyrk1A sequence. We generated the sh1073Dyrk1A and sc1073Dyrk1A by synthesizing two pairs of 54-mer oligonucleotides containing (1) a 20-nucleotide sense strand and a 20-nucleotide antisense strand, separated by a six-nucleotide loop (HindIII restriction site: AAGCTT); (2) a stretch of five timidines as a termination signal; and (3) 2G at the 5' and 3' ends. Sequence sh1073Dyrk1A (in italics,

¹Programa Gens i Malaltia. Centre de Regulació Genòmica-CRG, UPF, Parc de Recerca Biomèdica de Barcelona-PRBB, Barcelona 08003, Spain; ²Centro de Investigación Biomédica en Red de Enfermedades Raras, Barcelona 08003, Spain; ³Centro de Investigación Biomédica en Red de Epidemiología y Salud Pública, Barcelona 08003, Spain

*Correspondence: cristina.fillat@crge.es

DOI 10.1016/j.ajhg.2008.09.010. ©2008 by The American Society of Human Genetics. All rights reserved.

sense and antisense strands; underlined, loop) is as follows: sense oligonucleotide: 5'-GGGCAGAGGATATACAGTATAAGCTTATAC TGGTATATCCTCTGCCCTTTTTG-3'. Sequence sc1073Dyrk1A is as follows: sense oligonucleotide 5'-GGGCCCTCCATCACAGTCTA TAACCTTATAGACTGTGATGGAGGGCCCTTTTTG-3'. Sense and antisense oligonucleotides of each pair were annealed and cloned in the Apal and EcoRI sites of a modified pBluescript plasmid that contained the U6 promoter.¹³

Cell Culture and Transfection

HEK293 and COS-7 cells were plated at a density of 2×10^5 or 1×10^6 cells/well, respectively, in 60 mm dishes with Dulbecco's modified Eagle's medium (DMEM), supplemented with 5% fetal-calf serum (FCS) and antibiotics. Transfection of the different plasmids used in the study (pU6shDyrk1A, GFP-Dyrk1A, GFP-NHDyrk1A, and HA-RCAN1) was performed with Superfect Transfection Reagent (QIAGEN), in accordance with the manufacturer's instructions. Cells were harvested and processed 48 hr after transfection.

Primary Cell Culture

A primary culture of mouse cerebellar granule neurons (CGNs) was prepared as previously reported,¹⁴ with certain modifications. In brief, the cerebella of 7-day-old mouse pups were dissected in ice-cold Krebs's solution, diced, and dissociated with trypsin at 37°C. The dissociated cells were seeded at 3×10^5 cells/cm² onto a poly-L-lysine (Sigma)-coated culture dish (12-mm diameter; Becton Dickinson). Cells were cultured in DMEM supplemented with 10% FCS containing 25 mM KCl and were incubated at 37°C in humidified 5% CO₂. After 1 day in vitro (DIV 1), one volume of Neurobasal medium (Invitrogen), containing 25 mM KCl supplemented with 20 μM cytosine arabinoside (Ara-C) (Sigma), was added to the cultures. For preparation of the total cell extracts, CGNs were rinsed twice with PBS, collected in 100 μl of SDS-sample buffer, boiled for 10 min at 98°C, and analyzed with SDS-PAGE and immunoblotting.

Immunofluorescence

Cells were seeded at a density of 2×10^5 cells/well on sterile coverslips in 12-well plates and fixed in 4% paraformaldehyde. Cells were rinsed in PBS and permeabilized with PBS-0.1% Triton X-100 for 15 min at room temperature. Blocking was performed with PBS-10% FBS for 1 hr at room temperature. Then cells were incubated with rabbit anti-GFP (1:2500; Invitrogen) for 1 hr at room temperature, rinsed three times with PBS-0.1% Triton X-100-1% FBS and incubated with mouse anti-rabbit secondary antibody conjugated to FITC (1:100; Southern Biotechnologies) for 1 hr. Cells were then washed and mounted in a medium containing 0.2 μg/ml 4,6-diamidino-2-phenylindole (DAPI) for nuclear visualization (Vectashield, Vector). Preparations were visualized on a Leica DMR microscope. Images were taken with a Leica DC500 camera and processed on Leica IM1000 software.

Immunoblotting

Adult mouse striata homogenates and cell-culture extracts were obtained as follows: In brief, the striata were mechanically homogenized in a glass potter with a lysis buffer containing 320 mM sucrose, 50 mM Tris-HCl (pH 7.4), 10 mM EDTA, 1 mM PMSE, and protease inhibitor cocktail (Complete Mini, Roche). The homogenates were centrifuged for 10 min at 800 g at 4°C, and the supernatant was collected for further analysis. Primary granular neurons, HEK293 and COS-7 cells, were homogenized in 100 μl

lysis buffer (SDS 1% in PBS). Protein concentration was determined by a BCA assay (Pierce Biotechnology). Equal amounts of protein (80 and 30 μg for striata and cellular extracts, respectively) were loaded and separated on a 7.5% SDS-PAGE and were transferred onto nitrocellulose membranes (Amersham). Membranes were blocked with 5% nonfat milk in PBS-0.1% Tween-20 (PBS-T) solution and incubated overnight, with a polyclonal antibody against Dyrk1A (1:250)¹⁵ contained in the same incubation solution. The protein loading was monitored with a polyclonal antibody against β-Actin (1:2000; Sigma). Incubation with anti-rabbit or anti-mouse IgG/HRP (horseradish peroxidase) antibodies (1:2000; Dako) was performed for 1 hr at room temperature. Immunocomplexes were detected by chemiluminescence on an ECL detection system (Pierce), according to the manufacturer's instructions.

Recombinant Production of Adeno-Associated Viral Vector

The adeno-associated viral serotype 2 (AAV2) vectors used in the study were as follows: AAVshDyrk1A (expression cassette includes a hairpin-forming sequence against Dyrk1A gene under the control of the U6 promoter and the firefly luciferase gene under the control of the CMV promoter) and AAVscDyrk1A (expression cassette includes a hairpin-forming scrambled version obtained from the shDyrk1A sequence under the control of the U6 promoter and the firefly luciferase gene under the control of the CMV promoter). Both AAV2 vectors were produced in the Centre for Animal Biotechnology and Gene Therapy of the Universitat Autònoma de Barcelona (CBATEG-UAB) as previously described.¹⁶ The recombinant viruses were purified by iodixanol ultracentrifugation gradient and concentrated by application to an Amicon Ultra 100 kDa membrane. They were then resuspended in a PBS solution containing 1mM MgCl₂ and 2.5 mM KCl. The titers were AAVshDyrk1A (5.21×10^{11} genome copies/ml) and AAVscDyrk1A (5.25×10^{11} genome copies/ml).

AAV Infection of HEK293 Cells and CGNs

One day before infection, HEK293 cells or CGNs were seeded at a density of 1×10^3 or 1.25×10^5 cells/well, respectively, in 96-well plates. The virus was added to the medium at the indicated doses and removed 24 hr or 6 hr after infection (for the HEK293 cells and CGNs, respectively).

Quantification of Luciferase Expression

Luciferase transgene expression was measured in cell lysates or in the different brain areas in accordance with the manufacturer's instructions (Luciferase Assay System; Promega) and was normalized to total protein levels. An Orion microplate luminometer (Berthold Detection Systems) or a tube luminometer Autolumat Plus LB953 (Berthold) were respectively used to analyze the in vitro or in vivo samples. Protein concentration was determined with a BCA protein assay (Pierce Biotechnology). Results are expressed in RLU (relative light units, light units per μg protein).

Immunohistochemistry

Adult mice (3 to 10 months old) were deeply anaesthetized and perfused transcardially with cold PBS and subsequently with buffered 4% paraformaldehyde in PBS. After fixation, brains were removed from the skull and immersed in the same fixative overnight.

For luciferase and DARPP-32 detection, after rinsing in PBS, the brains were dehydrated and embedded in paraffin, and 5-μm-thick

sections were obtained with a sliding microtome (Leica). Sections were processed by the avidin-biotin-peroxidase method (Kit ABC, Dako), with a prior treatment in citrate buffer (pH 6.0) for antigen retrieval. After washing twice with water and PBS, the endogenous peroxidases were inactivated and tissue sections were incubated with blocking solution (PBS supplemented with 0.2% Triton X-100, 10% FBS, and 0.25% gelatine) for 1 hr at room temperature. Sections were then incubated overnight at 4°C with the primary monoclonal anti-DARPP-32 antibody (1:100; Cell Signaling), with the polyclonal anti-Luciferase antibody (1:1000; Sigma), or in the absence of primary antibody (for the negative control) in PBS with 0.2% Triton X-100 and 1% FBS. Subsequently, the sections were incubated with ABC solutions in accordance with the manufacturer's instructions. Peroxidase activity was visualized with 0.05% diaminobenzidine and 0.01% hydrogen peroxide. No immunoreaction was detected in the sections omitting the primary antibody, thus confirming the specificity of the reaction. All the sections were visualized on an Olympus microscope (Olympus BX51). Images were taken with an Olympus DP70 camera.

Animals

Transgenic mice (TgDyrk1A) overexpressing the full-length rat *Dyrk1A* cDNA under the control of the sheep metallothionein-1a promoter have been previously described by our group.¹⁰ TgDyrk1A mice were maintained as hemizygotes on a C57BL/6JXSJL background and housed under a 12:12 hr light-dark schedule (lights on at 8:00 a.m.) in controlled environmental conditions of humidity (60%) and temperature (22°C ± 2°C) with food and water ad libitum. The nontransgenic littermates of the TgDyrk1A mice served as controls. Only males were tested in this study. The number of animals used for each test was as follows: 14 mice/group (actimetry test), six mice/group (treadmill test), and seven mice/group (prepulse inhibition test). All the behavioral testing was conducted by the same experimenters, in an isolated room and at the same time of day. The behavioral experimenters were blinded as to the genetic and treatment status of the animals. All animal procedures met the guidelines of European Community Directive 86/609/EEC and were approved by the Local Ethics Committee.

Stereotaxic Injection

Adult (2- to 3-month-old) male TgDyrk1A and control mice were anesthetized with a combination of medetomidine (Domtor, Pfizer) and ketamine (Imalgene 500, Merial) at a dose of 1 mg/kg and 75 mg/kg, respectively. Then they were securely placed in a stereotaxic frame (Harvard Apparatus). The injections were performed bilaterally into the striatum at selected coordinates (AP +0.7 mm, L ± 2.0 mm, DV -3.0 mm relative to bregma) with a 5 µl Hamilton syringe. Three µl were injected per hemisphere at a rate of 0.2 µl/min in a two-step manner. Half the volume, 1.5 µl, was first injected at -3.00 mm DV, then the other half was injected at -2.5 mm DV. The rate of injection was precisely controlled by an infusion pump (Ultramicropump, World Precision Instruments). The needle was left in place for 5 min after the last injection and then slowly retracted from the brain. Before totally withdrawing, the needle was left in place for an additional 5 min. After the surgical intervention, animals were injected subcutaneously with a dose of 2 mg/kg of atipamezole (Antisedan, Pfizer) for anesthetic reversal. The analgesic buprenorphine (Buprex, Schering-Plough) was also administered intraperitoneally at a dose of 0.05 mg/kg every 8 hr for 48 hr after intervention.

When stated brains were sliced in 1-mm-width coronal sections with a Tissue Chopper (McIlwain, PANLAB S.L.)

In Vivo Bioluminescence

The luciferase activity was visualized with an in vivo bioluminescence imaging system (IVIS; Xenogen/Caliper Life Sciences). The images were captured and analyzed on Living Image 2.20.1 software (Xenogen/Caliper Life Sciences) and overlaid on Igor Pro 4.06A software (WaveMetrics). In brief, the animals were anesthetized and the substrate firefly D-luciferin (Xenogen/Caliper Life Sciences) was administered intraperitoneally (16 mg/kg). The bioluminescent images were acquired 14 min after administration of the substrate and after carrying out an initial optimization study. For the purpose of visualization, a light image of the animal was also taken and merged with the bioluminescent image with the software's overlay mode. This enabled the area of luciferase expression to be precisely correlated with the corresponding area of the mouse brain anatomy. The results are expressed as photons per second per square centimeter and per steradian.

Behavioral Analysis

Locomotor Activity

We measured locomotor activity by using actimetry boxes (45 × 45 cm; Harvard Apparatus) contained in a soundproof cupboard. Back and forward movements were monitored via a grid of infrared beams and used as an index of locomotor activity (counts). Counts were integrated every hour and added to obtain total locomotor activity for a 24 hr period maintaining the 12:12 hr light-dark schedule. The parameter measured in the present study was the total distance traveled by the animals (cm).

Treadmill Performance

The treadmill (Harvard Apparatus) consisted of a belt (50 cm long and 20 cm wide) that was run at a varying speed (5 to 150 cm⁻¹) and slope (0°–45°). At the end of the treadmill, there was an electrified grid that gave the mice a shock on the foot (0.4 mA) whenever they fell off the belt. Standard conditions were applied before intervention, consisting of the setting of consecutive trials of increasing difficulty (speed: 10, 20, 30, 40 cm⁻¹; slope: 20°). Forced conditions were applied after intervention, consisting of applying one single trial (speed: 60 cm⁻¹; slope: 40°). The cutoff time was at 1 min per trial. The order of presentation of the different belt speeds and slopes was identical for all mice. The mice were placed on the top of the already-moving belt, facing away from the electrified grid and in the opposite direction to the travel of the belt. Thus to avoid electric shocks the mice had to move forward. Whenever an animal fell from the belt, electrical shocks were applied to its paws for a maximum of 1 s. The results were processed with a one-way ANOVA statistical test.

Prepulse Inhibition of Startle Reflex

The apparatus used consisted of a chamber (Harvard Apparatus) containing a nonrestrictive cylindrical enclosure made of clear Plexiglas attached horizontally to a lightweight mobile platform that, in turn, rested on a solid base inside a sound-attenuated isolation cubicle. Acoustic noise bursts were presented via a speaker mounted 24 cm above the tube. Throughout the session, a background noise level of 70 db was maintained. A piezoelectric accelerometer mounted below the frame detected and transduced motion within the tube. Startle amplitudes were defined as the average of the stabilimeter readings collected from the onset of the stimulus. The mice were tested individually. Each mouse was put into the prepulse inhibition (PPI) chamber and, following a 5 min habituation period, submitted to a test session of 42 trials. Seven different types of trial

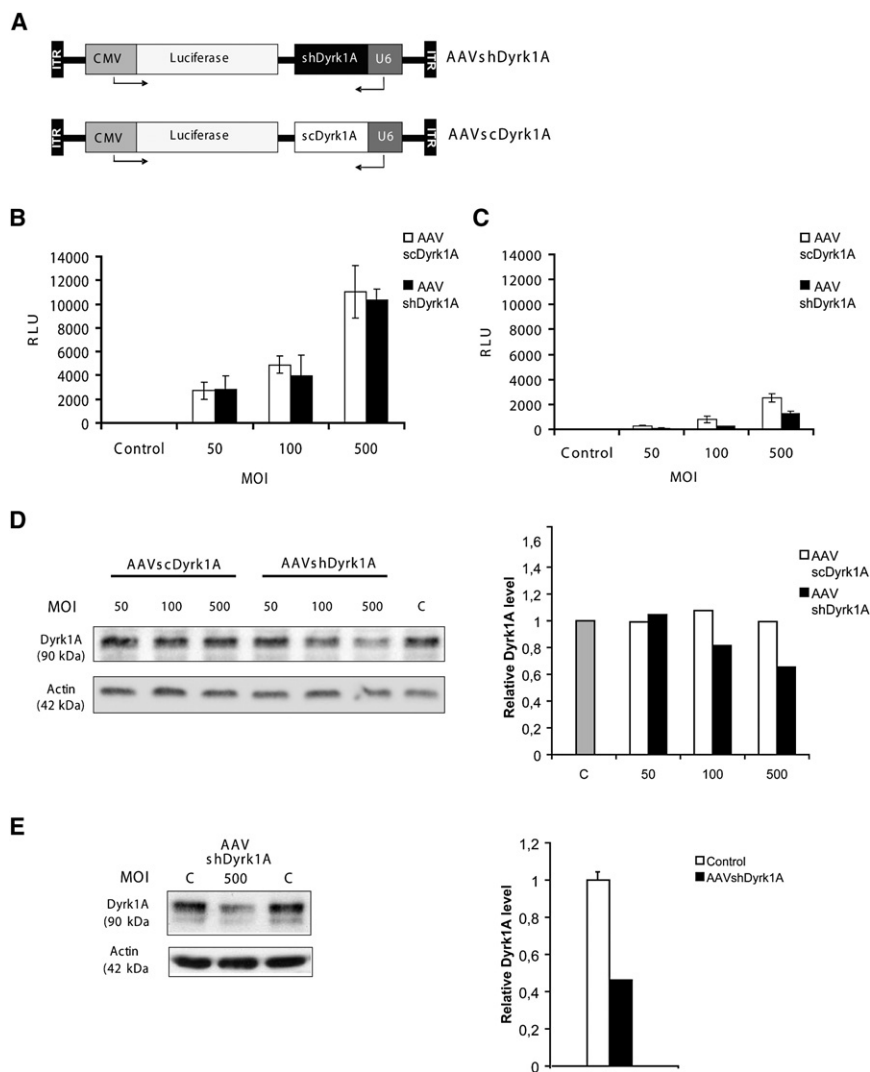


Figure 1. Generation and In Vitro Characterization of AAV-shRNA Targeting *Dyrk1A*

(A) Diagram of the recombinant AAV2/2 viral vectors containing the hairpin sequences under the control of the mouse U6 promoter and the firefly luciferase reporter gene under the control of the CMV promoter AAVshDyrk1A and AAVscDyrk1A. (B and C) Determination of luciferase activity in HEK293 cells (B) and primary cultures of CGNs (C) infected at 50, 100, and 500 MOI with the AAVshDyrk1A or AAVscDyrk1A virus. Data are expressed in relative light units (RLU or LU/ μ g). Values are expressed as mean \pm SEM of three independent experiments.

(D and E) Western blot showing Dyrk1A levels in control mock infected cultures (C) or after infection with 50, 100, and 500 MOI of AAVshDyrk1A and AAVscDyrk1A in HEK293 cells (D) or 500 MOI of AAVshDyrk1A in CGNs (E). Actin was used as an internal control. Bars show densitometric analysis of the Dyrk1A band normalized against the actin band.

the open reading frame, conserved in human, mouse, and rat *Dyrk1A*, encompassing nucleotides ranging from 1073 to 1092, 2002 to 2021, and 1132 to 1151 from the rat cDNA sequence. We constructed expression cassettes driving short hairpin RNA (shRNA) by the U6 promoter and

were used: no-stimulus trials, trials with an acoustic startle stimulus alone (120 dB), and trials in which a prepulse stimulus (74, 78, 82, 86, or 90 dB) was provided 100 ms prior to the startle stimulus. The different trials were presented in a random order, with an inter-trial interval of 15 s. The startle amplitude, defined as the peak response beginning at the onset of the startle stimulus, was measured for each trial. The levels of PPI at each prepulse sound level were calculated as $100 - [(response\ amplitude\ for\ prepulse-pulse\ stimulus / response\ amplitude\ for\ startle\ stimulus\ alone) \times 100]$.

Statistical Analysis

The statistical analysis on the behavioral studies was performed with one-way ANOVA whenever the factors were found to display significant interaction. Data are reported as mean \pm standard error of the mean (SEM). The statistical analysis was performed on SPSS 12.0 software. Student's *t* test was applied for evaluation of statistical significance in the luciferase assay. The cutoff point for significance was considered as $p < 0.05$.

Results

AAVshDyrk1A Reduces Dyrk1A Expression In Vitro

The targeting of Dyrk1A was designed in silico by the selection of three different 20-nucleotide target sequences of

screened in vitro them in order to identify the most efficient and specific shRNAs against Dyrk1A. Initially, the screening was performed in COS-7 cells cotransfected with the inhibitory plasmids and a plasmid encoding for GFP-Dyrk1A (Dyrk1A in-frame with the GFP). Western-blot and immunofluorescence analysis revealed the inhibitory effect of the sh1073Dyrk1A sequence; such an effect promoted a decrease in GFP-Dyrk1A protein expression. Conversely, neither the expression of the unrelated gene *RCAN1* or the truncated form of Dyrk1A (GFP-NHDyrk1A), lacking the target sequence for the sh1073RNA, were affected, indicating the specificity of sh1073Dyrk1A to the targeted sequence of Dyrk1A (Figure S1 available online).

The selected U6-sh1073RNA and its related scrambled control (sc) expression cassettes were cloned into AAV2 vectors (Figure 1A). We also modified the viral genome of the AAVs with the insertion of the firefly luciferase gene under the control of a CMV promoter to monitor cellular transduction. Infection of HEK293 cells and primary cultures of cerebellar granular neurons (CGN) showed a similar dose-response effect in the luciferase activity of both viruses (AAVsh Dyrk1A and AAVscDyrk1A). The

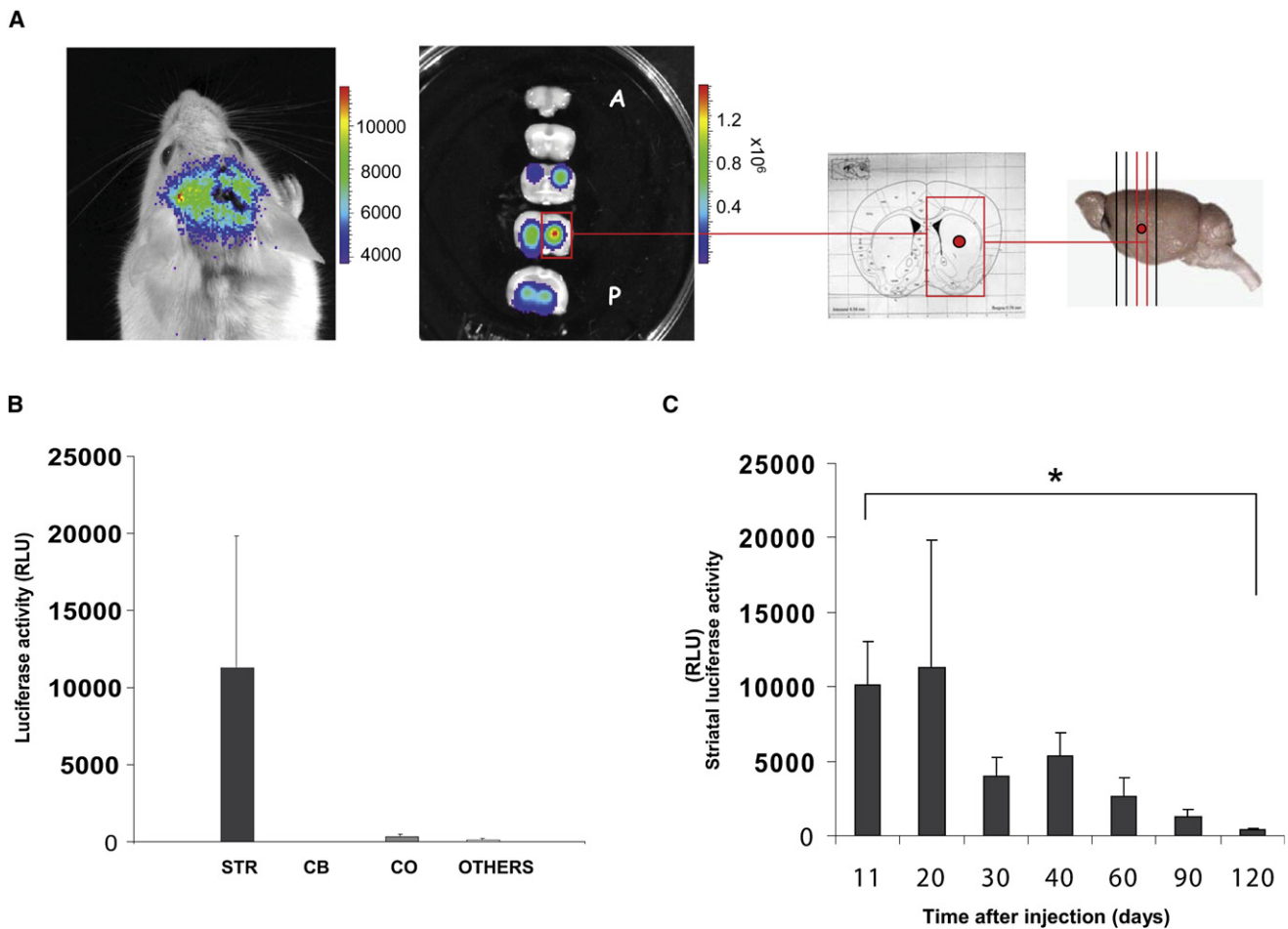


Figure 2. Follow-Up of Luciferase Expression after Intrastratial Injection of AAVshDyrk1A of TgDyrk1A Mice

(A) In vivo bioluminescence detection of luciferase activity in live animals and ex vivo sliced brains (slice width of 1 mm). Units are expressed as total photon counts. A viral dose of 1×10^9 vp in a 3 μ l total volume was injected per hemisphere. Red dot indicates stereotaxic injection coordinates. Animals were sacrificed 2 weeks after injection.

(B) Quantification of the luciferase activity present in the extracts of different brain areas 20 days after intrastratial injection of AAVsh-Dyrk1A (STR, striatum; CO, cortex; CB, cerebellum). Data are expressed in RLU. Values are expressed as mean \pm SEM ($n = 4$ mice).

(C) Time course of luciferase expression after intrastratial administration of AAVshDyrk1A. Animals were sacrificed at different days after intervention. Data are given in RLU. Values are expressed as mean \pm SEM ($n = 4$ mice). The asterisk indicates significance with a p value < 0.05.

transduction efficiency was higher in the HEK293 cells than in the CGNs, as detected by luciferase-activity measurement (Figures 1B and 1C). The inhibitory efficiency of the AAVshDyrk1A was assessed by western-blot analysis, showing that AAVshDyrk1A, but not control AAVsc-Dyrk1A, reduced endogenous Dyrk1A protein expression in HEK293 cells in a dose-response manner (Figure 1D). An inhibitory effect of the AAVshDyrk1A was also observed in mouse CGNs, although a higher viral dose of 500 MOIs was required (Figure 1E).

AAVshDyrk1A Gene Transfer to the Striatum Reduces Dyrk1A Gene Expression

We next investigated whether the viral particles generated were capable of efficiently infecting the striatum of TgDyrk1A mice. Taking advantage of the fact that both viruses contained a luciferase reporter, we monitored the

levels, biodistribution, and kinetics of the viral infections with in vivo bioluminescence and by biochemically determining luciferase activity in brain extracts. Bioluminescent measurement of the light emitted in live mice, 2 weeks after viral injection, showed efficient transduction of the viral particles. Luciferase expression extended up to 2 mm along the rostrocaudal axes, as shown by the analysis of 1-mm-thick coronal brain sections (Figure 2A). Indeed, luciferase activity was mostly restricted to the brain area corresponding to the striatum (Figure 2B). Kinetic studies showed that luciferase expression peaked between 10 to 20 days after injection and significantly decreased 4 months later (Figure 2C). This reduction in luciferase expression could probably be related to the described epigenetic inactivation of the CMV promoter and independent of viral transduction.¹⁷ In fact, western-blot analysis of Dyrk1A indicated that Dyrk1A levels in the striatum of

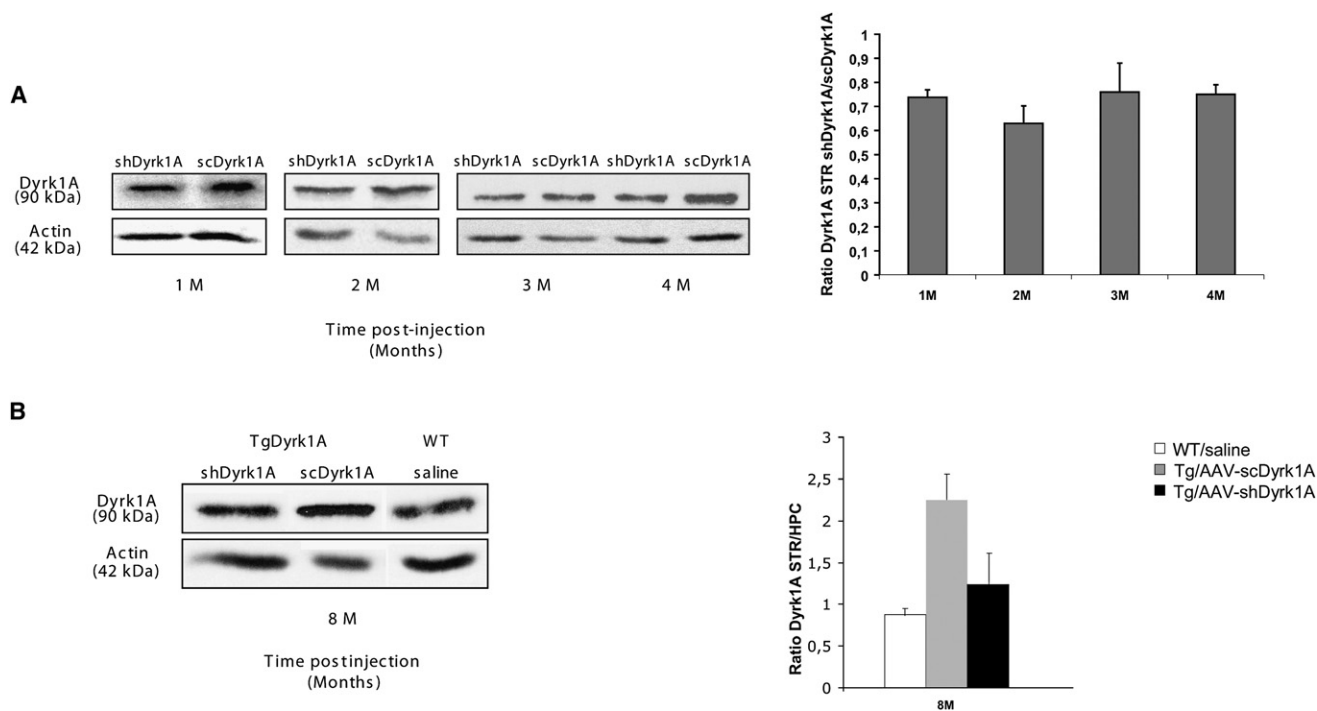


Figure 3. Kinetics of Dyrk1A Inhibition in the Striatum of TgDyrk1A Mice after AAVshDyrk1A Administration
 Western-blot analysis of Dyrk1A protein levels. (A) shows representative images of Dyrk1A expression from striata ipsilaterally injected with AAVshDyrk1A and contralaterally injected with AAVscDyrk1A at 1, 2, 3, and 4 months after injection. Bars show densitometric analysis of the Dyrk1A band, normalized against the actin band and represented as the ratio of shDyrk1A versus scDyrk1A signal. Data are expressed as the mean \pm SEM ($n = 4$ mice). (B) shows a representative western blot of Dyrk1A expression from TgDyrk1A striata injected with AAVshDyrk1A or with AAVscDyrk1A and from wild-type mice injected with saline. Bars show densitometric analysis of Dyrk1A signal from striata normalized to Dyrk1A hippocampal levels. Data are expressed as the mean \pm SEM ($n = 4$ mice). Actin was used as an internal control.

TgDyrk1A mice injected with AAVshDyrk1A were efficiently reduced *in vivo* at all the time points analyzed (Figure 3A). Interestingly, this inhibitory effect was still present 8 months after AAVshDyrk1A injections in TgDyrk1A mice striata, with a reduction of Dyrk1A to levels that were similar to those of wild-type animals (Figures 3B and 3C).

Although the use of adeno-associated vectors is virtually devoid of toxicity to the central nervous system, putative neurotoxicity associated to shRNA sequences has recently been reported.¹⁸ To examine any striatal damage, we performed an immunohistochemical analysis of the dopamine and cAMP-regulated phosphoprotein (DARPP-32), a marker of medium-sized spiny-projection neurons in the striatum, reported as an indicator of shRNA toxicity in the striatum,¹⁸ in coronal sections of AAVshDyrk1A-treated mice, harvested at 2 weeks and 8 months after intervention. No differences in DARPP-32 immunoreactivity were observed when we compared the DARPP-32 signal of the hemisphere injected with AAVshDyrk1A to that of the contralateral, which received saline solution alone (Figure 4). Luciferase-positive cells were immunostained in the AAVshDyrk1A hemisphere, indicating viral transduction (Figure 4). No changes in DARPP-32 immunoreactivity were observed in the striatum of the saline-,

AAVscDyrk1A-, and AAVshDyrk1A-treated mice 8 months after intervention (data not shown).

Striatal Delivery of AAVshDyrk1A Attenuates Motor Alterations in Adult TgDyrk1A Mice

To investigate the effects of inhibiting Dyrk1A overexpression in the case of established TgDyrk1A motor deficits, we injected AAVshDyrk1A into the striatum of 2- to 3-month-old adult TgDyrk1A mice and performed behavioral phenotyping at preinjection and different postinjection time points. TgDyrk1A mice were randomly assigned to three groups bilaterally receiving AAVshDyrk1A, AAVscDyrk1A, or saline, along with a group of wild-type mice injected with saline. Circadian activity under basal conditions was assessed by the actimetry box test. In preinjection sessions, although no differences were observed in the circadian rhythms, TgDyrk1A mice showed a greater total distance traveled in 24 hr compared to that of wild-type mice, indicating a hyperactive phenotype (Figure 5A; $p < 0.05$; $n = 14$). Two months after intervention, a reduction in hyperactive behavior was observed only in the TgDyrk1A mice injected with AAVshDyrk1A. Their total activity was lower than that of the TgDyrk1A mice injected with saline alone (Figure 5A; $p < 0.05$; $n = 14$) or with AAVscDyrk1A (Figure 5A; $p = 0.09$). Importantly, 4 months after injection,

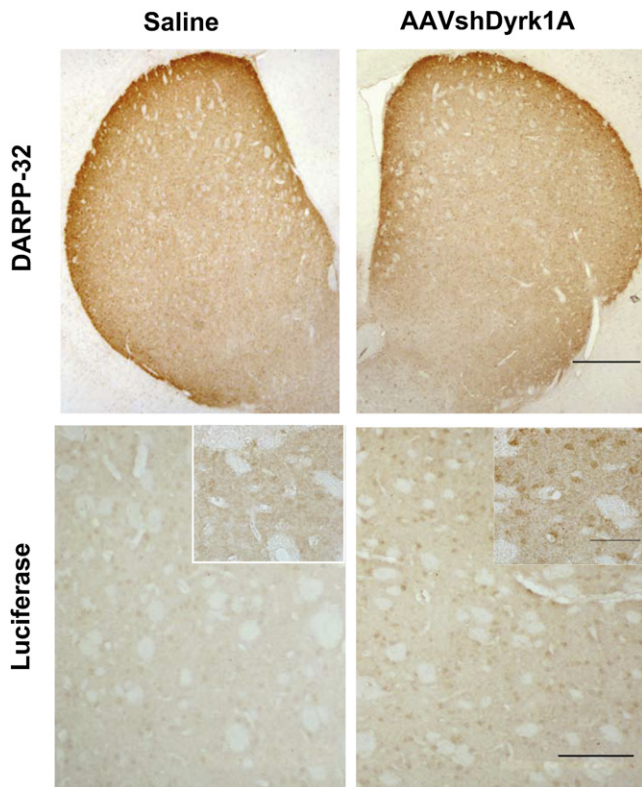


Figure 4. Analysis of AAVshDyrk1A Striatal Toxicity

Animals were stereotaxically injected with saline in the striata ipsilateral hemisphere and with AAVshDyrk1A in the contralateral hemisphere. Immunohistochemical staining of DARPP-32 and luciferase was performed on coronal sections of brains harvested 2 weeks after injection, with an anti-DARPP32 monoclonal and anti-luciferase polyclonal antibody, respectively. Representative photomicrographs of DARPP-32-positive medium spiny neurons (upper panel) and luciferase-positive neurons (lower panel) are shown. The scale bar represents 1 mm for the upper panel and 200 μm for the lower panel (100 μm for higher magnification).

a far more significant reduction in activity was observed in the TgDyrk1A mice treated with AAVshDyrk1A than in those treated either with AAVscDyrk1A ($p < 0.01$) or saline ($p < 0.05$) (Figure 5A; $n = 14$), thereby achieving levels of activity similar to those detected in wild-type mice thus indicating a complete reversal of hyperactivity by Dyrk1A expression normalization.

Next, we investigated the effects of AAVshDyrk1A treatment on motor coordination of TgDyrk1A mice that was previously demonstrated to be significantly affected by using a treadmill test.⁸ TgDyrk1A mice performed the task significantly worse than wild-type mice, as revealed by the higher number of shocks received (Figure 5B; $p < 0.005$; $n = 6$). When mice were submitted to the task at 1 month after treatment, at 40° slope and a speed of 60 cm^{-1} , TgDyrk1A mice injected with AAVshDyrk1A showed a significant improvement in the performance of the task, as reflected by the fact that they received less shocks than the TgDyrk1A mice injected either with AAVscDyrk1A ($p < 0.05$) or saline ($p < 0.05$). The AAVshDyrk1A-treated mice

performed the task at a similar level to that of the saline-injected wild-type mice (Figure 5B; $n = 6$). In these groups of mice, higher-demanding conditions had to be applied because of the habituation and learning effect detected when we used the same experimental conditions. Notably, this amelioration in motor-coordination skills was likewise observed 4 months after intervention, when the animals were sacrificed (Figure 5B; $p < 0.05$; $n = 6$).

The striatum forms part of the cortico-striato-pallidal circuitry, also involved in sensorimotor gating.¹⁹ To assess any possible deficits in this function, we measured the levels of the PPI mechanism, an operational measure of sensorimotor gating.²⁰ TgDyrk1A mice showed a decrease in PPI levels that was more pronounced at the higher prepulse intensities used. These results suggested the presence of deficits in sensorimotor gating, although the differences did not reach statistical significance (Figure 5C; $n = 7$). When we repeated the test 4 months after injection, we observed an important increase in the PPI levels of the group of TgDyrk1A mice that had received AAVshDyrk1A, as compared to those of the AAVscDyrk1A-treated group. The increase was significant at the prepulse intensities of 74 dB and 86 dB (Figure 5D; $p < 0.05$; $n = 7$). Furthermore, the TgDyrk1A mice that received AAVshDyrk1A were the only treated group that showed a significant improvement in PPI at the different time point analyzed, achieving statistical significance 2 and 4 months after the intervention at a prepulse intensity of 78 dB (Figure 5E; $p < 0.05$; $n = 7$).

Discussion

Viral delivery of shRNA candidates presents an alternative approach to mouse genetic engineering with which to understand pathophysiology and test potential therapeutic targets. In the present study, we demonstrate that AAVshRNA strategies are an effective way to study the impact of single-gene downregulation in adult mice, within the context of phenotypes deriving from nonmutated gene overexpression. We demonstrate that intrastriatal injections of AAVshDyrk1A in TgDyrk1A mice normalize Dyrk1A gene expression in the striatum and correct established motor alterations.

The efficacy of such approach in normalizing Dyrk1A content in TgDyrk1A mice probably resulted from both, the use of the AAV2 serotype virus that stably transduces neuronal cells in the striatum at a moderate efficiency and the selected applied dose of 10^9 viral genomes per hemisphere.

It is worth noting that, to our knowledge, this is the first study that demonstrates effective in vivo correction of an RNAi approach in a mouse model that displays Down syndrome-related phenotypes.

To date, few studies have shown a potential to rescue DS phenotypes, and all have been based on pharmacological intervention in mouse models. It has recently been shown that chronic treatment with GABA antagonists in Ts65Dn

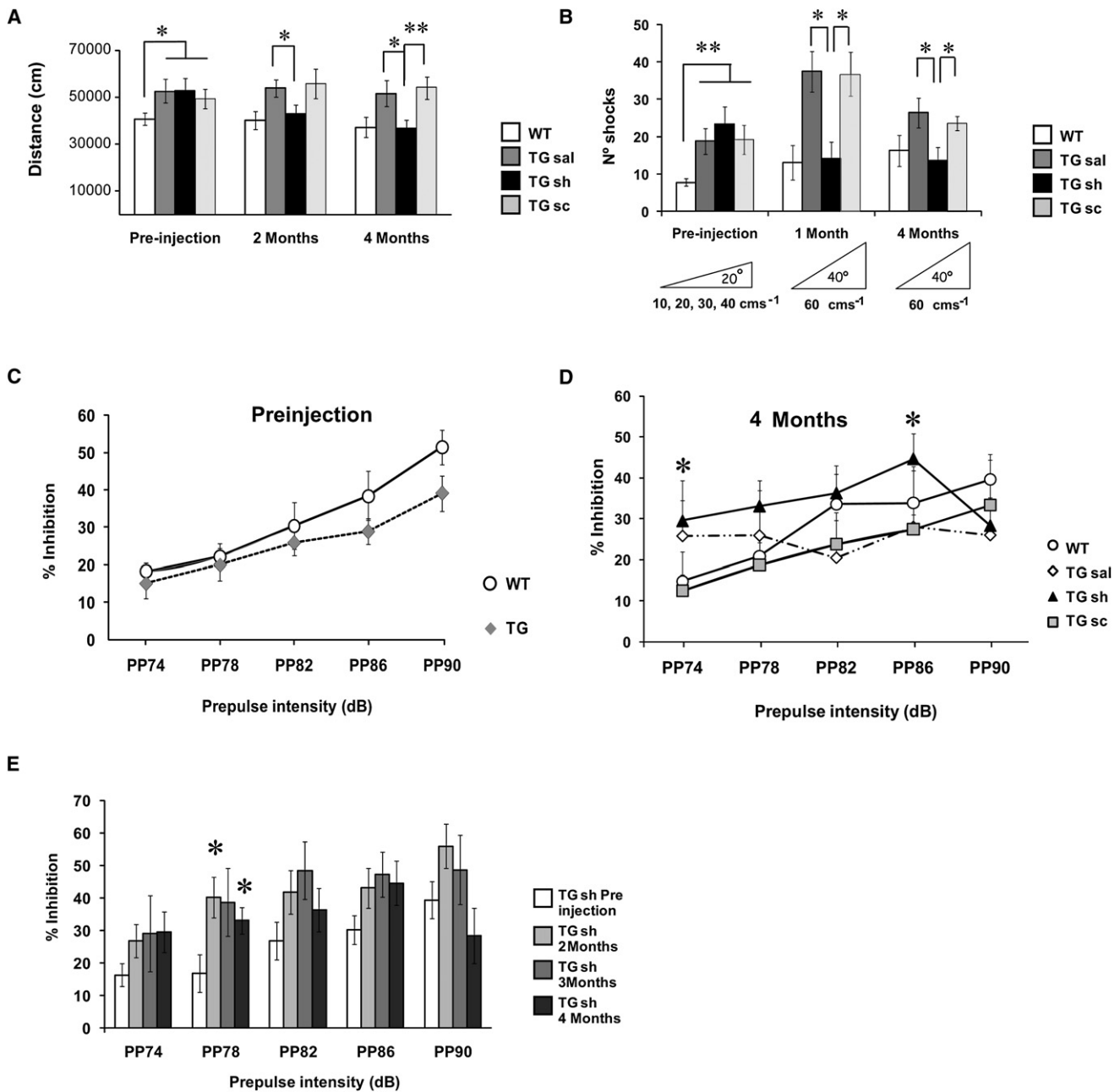


Figure 5. Behavioral Analysis of Motor Tasks in TgDyrk1A Treated with Intrastratial Injections of AAVshDyrk1A

Animals were randomly assigned to four treatment groups: wild-type (saline) and TgDyrk1A (saline, AAVshDyrk1A, and AAVscDyrk1A). (A) Actimetry test. The results are given as total distance traveled by the animals in 24 hr expressed in cm. Preinjection results confirmed the hyperactive phenotype of TgDyrk1A mice compared to the control group ($F_{1,52} = 4.898$, $*p = 0.031$). Two months after the intervention, a decrease in the hyperactivity was observed in TgDyrk1A mice injected with AAVshDyrk1A (TG sh) with respect to saline (TG sal), ($F_{1,23} = 4.286$, $*p = 0.05$). This reduction became more evident when repeating the test 4 months after treatment (TG sal versus TG sh: $F_{1,24} = 5.225$, $*p = 0.032$; TG sc versus TG sh: $F_{1,23} = 9.05$, $**p = 0.006$), ($n = 14$ mice/group).

(B) Treadmill test. The results are expressed as the total number of shocks received. Nontreated mice confirmed the presence of motor-coordination alterations in TgDyrk1A mice ($F_{1,22} = 11.937$, $**p = 0.002$). One month after the intervention, the AAVshDyrk1A TgDyrk1A group received a significantly less number of shocks compared to the groups of TgDyrk1A injected with either saline or AAVscDyrk1A, reaching levels similar to those of control groups (TG sal versus TG sh: $F_{1,6} = 8.669$, $*p = 0.032$; TG sc versus TG sh: $F_{1,8} = 9.844$, $*p = 0.016$). This effect was maintained 4 months after treatment in AAV-shDyrk1A TgDyrk1A mice (TG sal versus TG sh: $F_{1,10} = 5.575$, $*p = 0.043$; TG sc versus TG sh: $F_{1,10} = 6.094$, $*p = 0.033$), ($n = 6$ mice/group).

(C–E) Prepulse inhibition (PPI) test. Results are expressed as the percentage of inhibition, that refers to the decrease in the amplitude of the startle response to a given acoustic pulse (120 dB) when it is preceded by a prepulse (74, 78, 82, 86, and 90 dB). As shown in (C), results before the intervention indicated deficits in the PPI in TgDyrk1A mice, as shown by a tendency to decreased PPI at higher prepulse intensities. As shown in (D), 4 months after the injection, AAVshDyrk1A TgDyrk1A showed a statistically significant increase in PPI at

mice, a trisomy model of DS, leads to a recovery of cognition and long-term potentiation phenotypes, indicating that the intellectual disabilities associated with DS could potentially be corrected.²¹ Improvement in the behavioral performance of Ts65Dn mice in a learning and memory test after an acute injection of the uncompetitive NMDAR antagonist memantine has also been recently recorded.²² Despite the great relevance of the above data, there is currently no treatment that specifically aims to normalize the gene expression levels of critical aneuploidy genes.

With the approach described in the current study, we have defined the association of the normalization of Dyrk1A protein levels with the rescue of the motor phenotype. It should be noted that the effect was found to be long-lasting, because it was still significant eight months after injection, thus suggesting that the phenotype amelioration achieved could indeed be far longer lasting. In fact, the improved performance in the activity test was more significant at 4 than at 2 months after treatment, suggesting that prolonged Dyrk1A normalized expression facilitates the correction of striatal-dependent phenotypes. Importantly, the AAVshDyrk1A therapy administered was well tolerated as evidenced by the lack of neurotoxicity to the tested shRNA sequences targeting Dyrk1A and to the absence of any deleterious effect due to the reduction in Dyrk1A expression in TgDyrk1A mice striatum.

The above data offer further support to the notion that Dyrk1A plays an important role in the control of motor activity. The participation of Dyrk1A in motor physiology first came to light with the behavioral analysis of different models of Dyrk1A-dosage imbalance. TgDyrk1A mice present motor abnormalities in the areas of coordination and motor learning, with the organization of motor behavior being the area most severely affected.^{8,10} On the other hand, the haploinsufficient murine model *Dyrk1A+/-*, which presents reduced levels of Dyrk1A, has been shown to present hypoactivity^{23,24} similar to that of the mutant flies of Dyrk1A orthologous gene *Drosophila mnb*.²⁵ Recently, the truncation of Dyrk1A in a patient has also been associated to a delay in gross motor development.²⁶ Although it is generally believed that these phenotypes might derive from aberrant brain development, the motor phenotype rescue in adult mice observed in our study would suggest an active role for Dyrk1A in the neural processes that take place in the mature brain. The current study also highlights the contribution of the striatum to the motor phenotype of TgDyrk1A mice. In this respect, Dyrk1A has been shown to be highly expressed in the adult mice striatum, indicating that the kinase may play an important role in such structure.²⁷ Moreover, recent observations have shown that the correct levels of Dyrk1A are essential to the proper functioning of the nigrostriatal

dopaminergic neurons,²⁸ which are thought to play a key role in modulating excitatory neurotransmission in motor circuitry.²⁹

Therefore, the results obtained in the present study demonstrate that the normalization of Dyrk1A gene expression reverses the motor phenotypes of transgenic Dyrk1A mice.

This strategy provides a proof of concept on the Dyrk1A-phenotype dependency. In principle, it could be speculated that the spatial-learning phenotype also present in these mice could be rescued by applying a similar approach with adequate AAV serotypes targeting the hippocampus. On the other hand, it is clear that the real potential of the present strategy is yet to be investigated in the trisomic context in the existing partial trisomic mouse models. In this case, if Dyrk1A is a major candidate gene in motor and learning phenotypes, its normalization could also have beneficial effects. However we have to bear in mind that in the trisomic context, many other genes are overexpressed that may influence on the normalization effects. Moreover, the strategy developed in the current work can be further applied to identify the role of additional genes that might be considered therapeutic targets in Down syndrome.

Supplemental Data

Supplemental Data include one figure and can be found with this article online at <http://www.ajhg.org/>.

Acknowledgments

This work has been supported by grants from Spanish Ministry of Health (FIS PI041559), Jérôme Lejeune Foundation, EU FP6-2005-LIFESCIHEALTH-6 ANEUPLOIDY No.037627. The CIBER de Enfermedades Raras is an initiative of the ISCIII. X.A. is partially financed by the Instituto de Salud Carlos III (CP07/00323). We acknowledge the UPV-CBATEG and the Association Française contre les Myopathies for the AAV vector production.

Received: July 25, 2008

Revised: September 17, 2008

Accepted: September 17, 2008

Published online: October 9, 2008

References

1. Hattori, M., Fujiyama, A., Taylor, T.D., Watanabe, H., Yada, T., Park, H.S., Toyoda, A., Ishii, K., Totoki, Y., Choi, D.K., et al. (2000). The DNA sequence of human chromosome 21. *Nature* 405, 311–319.
2. Antonarakis, S.E., and Epstein, C.J. (2006). The challenge of Down syndrome. *Trends Mol. Med.* 12, 473–479.
3. Dowjat, W.K., Adayev, T., Kuchna, I., Nowicki, K., Palmieriello, S., Hwang, Y.W., and Wegiel, J. (2007). Trisomy-driven

74 dB and 86 dB prepulse intensities (TG sc versus TG sh; $F_{1,14} = 5.55$, $*p = 0.035$; $F_{1,14} = 5.234$, $*p = 0.04$). As shown in (E), comparisons of the AAVshDyrk1A-injected group at the indicated time points showed significant differences (TG sh Preinjection versus TG sh, 2 months: $F_{1,13} = 7.449$, $*p = 0.018$; Preinjection versus TG sh, 4 months: $F_{1,13} = 5.207$, $*p = 0.042$), ($n = 7$ mice/group). Data are expressed as means \pm SEM.

- overexpression of DYRK1A kinase in the brain of subjects with Down syndrome. *Neurosci. Lett.* *413*, 77–81.
4. Guimera, J., Casas, C., Estivill, X., and Pritchard, M. (1999). Human minibrain homologue (MNBH/DYRK1): Characterization, alternative splicing, differential tissue expression, and overexpression in Down syndrome. *Genomics* *57*, 407–418.
 5. Becker, W., Weber, Y., Wetzell, K., Eirnbter, K., Tejedor, F.J., and Joost, H.G. (1998). Sequence characteristics, subcellular localization, and substrate specificity of DYRK-related kinases, a novel family of dual specificity protein kinases. *J. Biol. Chem.* *273*, 25893–25902.
 6. Dierssen, M., and de Lagran, M.M. (2006). DYRK1A (dual-specificity tyrosine-phosphorylated and -regulated kinase 1A): A gene with dosage effect during development and neurogenesis. *ScientificWorldJournal* *6*, 1911–1922.
 7. Smith, D.J., Stevens, M.E., Sudanagunta, S.P., Bronson, R.T., Makhinson, M., Watabe, A.M., O'Dell, T.J., Fung, J., Weier, H.U., Cheng, J.F., et al. (1997). Functional screening of 2 Mb of human chromosome 21q22.2 in transgenic mice implicates minibrain in learning defects associated with Down syndrome. *Nat. Genet.* *16*, 28–36.
 8. Martinez de Lagran, M., Altafaj, X., Gallego, X., Marti, E., Estivill, X., Sahun, I., Fillat, C., and Dierssen, M. (2004). Motor phenotypic alterations in TgDyrk1a transgenic mice implicate DYRK1A in Down syndrome motor dysfunction. *Neurobiol. Dis.* *15*, 132–142.
 9. Ahn, K.J., Jeong, H.K., Choi, H.S., Ryoo, S.R., Kim, Y.J., Goo, J.S., Choi, S.Y., Han, J.S., Ha, I., and Song, W.J. (2006). DYRK1A BAC transgenic mice show altered synaptic plasticity with learning and memory defects. *Neurobiol. Dis.* *22*, 463–472.
 10. Altafaj, X., Dierssen, M., Baamonde, C., Marti, E., Visa, J., Guimera, J., Oset, M., Gonzalez, J.R., Florez, J., Fillat, C., et al. (2001). Neurodevelopmental delay, motor abnormalities and cognitive deficits in transgenic mice overexpressing Dyrk1A (minibrain), a murine model of Down's syndrome. *Hum. Mol. Genet.* *10*, 1915–1923.
 11. Arron, J.R., Winslow, M.M., Polleri, A., Chang, C.P., Wu, H., Gao, X., Neilson, J.R., Chen, L., Heit, J.J., Kim, S.K., et al. (2006). NFAT dysregulation by increased dosage of DSCR1 and DYRK1A on chromosome 21. *Nature* *441*, 595–600.
 12. Warrington, K.H., Jr., and Herzog, R.W. (2006). Treatment of human disease by adeno-associated viral gene transfer. *Hum. Genet.* *119*, 571–603.
 13. Sui, G., Soohoo, C., Affar el, B., Gay, F., Shi, Y., and Forrester, W.C. (2002). A DNA vector-based RNAi technology to suppress gene expression in mammalian cells. *Proc. Natl. Acad. Sci. USA* *99*, 5515–5520.
 14. Fujita, Y., Katagi, J., Tabuchi, A., Tsuchiya, T., and Tsuda, M. (1999). Coactivation of secretogranin-II and BDNF genes mediated by calcium signals in mouse cerebellar granule cells. *Brain Res. Mol. Brain Res.* *63*, 316–324.
 15. Marti, E., Altafaj, X., Dierssen, M., de la Luna, S., Fotaki, V., Alvarez, M., Perez-Riba, M., Ferrer, I., and Estivill, X. (2003). Dyrk1A expression pattern supports specific roles of this kinase in the adult central nervous system. *Brain Res.* *964*, 250–263.
 16. Salvetti, A., Oreve, S., Chadeuf, G., Favre, D., Cherel, Y., Champion-Arnaud, P., David-Ameline, J., and Moullier, P. (1998). Factors influencing recombinant adeno-associated virus production. *Hum. Gene Ther.* *9*, 695–706.
 17. Brooks, A.R., Harkins, R.N., Wang, P., Qian, H.S., Liu, P., and Rubanyi, G.M. (2004). Transcriptional silencing is associated with extensive methylation of the CMV promoter following adenoviral gene delivery to muscle. *J. Gene Med.* *6*, 395–404.
 18. McBride, J.L., Boudreau, R.L., Harper, S.Q., Staber, P.D., Monteys, A.M., Martins, I., Gilmore, B.L., Burstein, H., Peluso, R.W., Polisky, B., et al. (2008). Artificial miRNAs mitigate shRNA-mediated toxicity in the brain: Implications for the therapeutic development of RNAi. *Proc. Natl. Acad. Sci. USA* *105*, 5868–5873.
 19. Campbell, L.E., Hughes, M., Budd, T.W., Cooper, G., Fulham, W.R., Karayanidis, F., Hanlon, M.C., Stojanov, W., Johnston, P., Case, V., et al. (2007). Primary and secondary neural networks of auditory prepulse inhibition: A functional magnetic resonance imaging study of sensorimotor gating of the human acoustic startle response. *Eur. J. Neurosci.* *26*, 2327–2333.
 20. Geyer, M.A., Krebs-Thomson, K., Braff, D.L., and Swerdlow, N.R. (2001). Pharmacological studies of prepulse inhibition models of sensorimotor gating deficits in schizophrenia: A decade in review. *Psychopharmacology (Berl.)* *156*, 117–154.
 21. Fernandez, F., Morishita, W., Zuniga, E., Nguyen, J., Blank, M., Malenka, R.C., and Garner, C.C. (2007). Pharmacotherapy for cognitive impairment in a mouse model of Down syndrome. *Nat. Neurosci.* *10*, 411–413.
 22. Costa, A.C., Scott-McKean, J.J., and Stasko, M.R. (2008). Acute injections of the NMDA receptor antagonist memantine rescue performance deficits of the Ts65Dn mouse model of Down syndrome on a fear conditioning test. *Neuropsychopharmacology* *33*, 1624–1632.
 23. Fotaki, V., Dierssen, M., Alcantara, S., Martinez, S., Marti, E., Casas, C., Visa, J., Soriano, E., Estivill, X., and Arbones, M.L. (2002). Dyrk1A haploinsufficiency affects viability and causes developmental delay and abnormal brain morphology in mice. *Mol. Cell. Biol.* *22*, 6636–6647.
 24. Fotaki, V., Martinez De Lagran, M., Estivill, X., Arbones, M., and Dierssen, M. (2004). Haploinsufficiency of Dyrk1A in mice leads to specific alterations in the development and regulation of motor activity. *Behav. Neurosci.* *118*, 815–821.
 25. Tejedor, F., Zhu, X.R., Kaltenbach, E., Ackermann, A., Baumann, A., Canal, I., Heisenberg, M., Fischbach, K.F., and Pongs, O. (1995). minibrain: A new protein kinase family involved in postembryonic neurogenesis in *Drosophila*. *Neuron* *14*, 287–301.
 26. Moller, R.S., Kubart, S., Hoeltzenbein, M., Heye, B., Vogel, I., Hansen, C.P., Menzel, C., Ullmann, R., Tommerup, N., Ropers, H.H., et al. (2008). Truncation of the Down syndrome candidate gene DYRK1A in two unrelated patients with microcephaly. *Am. J. Hum. Genet.* *82*, 1165–1170.
 27. Okui, M., Ide, T., Morita, K., Funakoshi, E., Ito, F., Ogita, K., Yoneda, Y., Kudoh, J., and Shimizu, N. (1999). High-level expression of the Mnb/Dyrk1A gene in brain and heart during rat early development. *Genomics* *62*, 165–171.
 28. Martinez de Lagran, M., Bortolozzi, A., Millan, O., Gispert, J.D., Gonzalez, J.R., Arbones, M.L., Artigas, F., and Dierssen, M. (2007). Dopaminergic deficiency in mice with reduced levels of the dual-specificity tyrosine-phosphorylated and regulated kinase 1A, Dyrk1A(+/-). *Genes Brain Behav.* *6*, 569–578.
 29. Hallett, P.J., Spoelgen, R., Hyman, B.T., Standaert, D.G., and Dunah, A.W. (2006). Dopamine D1 activation potentiates striatal NMDA receptors by tyrosine phosphorylation-dependent subunit trafficking. *J. Neurosci.* *26*, 4690–4700.